J. F. Snape[1*], A. A. Nemchin[1,2], M. L. Grange[2], J. J. Bellucci[1], F. Thiessen[1], M. J. Whitehouse[1]

*Corresponding author, email address: Joshua.snape@nrm.se

[1]Department of Geosciences, Swedish Museum of Natural History, SE-104 05 Stockholm, Sweden

[2]Department of Applied Geology, Curtin University, Perth, WA 6845, Australia

Phosphate ages in Apollo 14 breccias: Resolving multiple impact events with high precision U-Pb SIMS analyses

Abstract

The U-Pb systems of apatite and merrillite grains within four separate Apollo 14 impact melt breccia samples were analysed by secondary ion mass spectrometry. No systematic difference was identified between the $^{207}Pb/^{206}Pb$ ages of the apatites and merrillites. A combined $^{207}Pb/^{206}Pb$ age of 3927±2 Ma (95% conf.) is determined for three of these samples (14305,103: 3926±4 Ma; 14306,150: 3926±6 Ma; 14314,13: 3929±4 Ma). By combining these data with the ages previously obtained for zircons in Apollo 12 impact melt breccia fragments and the lunar meteorite SaU 169, a weighted average age of 3926±2 Ma (95% conf.) is obtained, which is attributed to the formation of the Imbrium basin. An age of 3943±5 Ma is determined for the fourth breccia (14321,134), which is similar to ages of 3946±15 Ma and 3958±19 Ma, obtained from several older phosphates in 14305,103 and 14314,13. The weighted average of these three older ages is 3944±4 Ma (95% conf.). This is indistinguishable to the age (3938±4 Ma; 2σ) obtained for a different Apollo 14 impact melt breccia in a previous study. After investigating likely sources for this older ~3940 Ma age, we conclude that the Humorum or Serenitatis basin forming events are likely candidates. The potential identification of two large impact events within ~15 Myrs has important implications for the rate of lunar bombardment around 3.95-3.92 Ga. This study demonstrates the importance of high-precision age determinations for interpreting the impact record of the Moon, as documented in lunar samples.

1. Introduction

Constraining the impact history of the Moon is a key priority, both for lunar science (NRC 2007) and also for our understanding of the fundamental geologic processes (e.g. Melosh 1989) that affected the evolution of planets in the inner Solar System. One aspect of understanding the lunar impact record is testing the concept that there was a period of intense meteoritic bombardment occurring at approximately 3.9 Ga, which was initially developed on the basis of similar ages being identified for multiple Apollo samples (Turner et al. 1973; Tera et al. 1974). Subsequent studies have led to the development of several contemporary models, suggesting varying degrees of intensity and duration of early inner Solar System bombardment (e.g. Ryder 1990; Morbidelli et al. 2012; Marchi et al. 2014). A significant challenge in obtaining evidence for these models is the relatively limited range of locations visited by the Apollo and Luna missions, and the possibility that these sites are dominated by material originating from a few large impact basins (Wetherill 1981; Cohen et al. 2000; Baldwin 2006; Fig. 1). The Apollo 14 landing site, for example, has been interpreted as consisting primarily of material ejected from the Imbrium basin, (i.e. the Fra Mauro Formation; Swann et al. 1971; 1977). However, the remoteness of the landing site from the basin (600-800 km from the rim of the Imbrium basin) combined with the disruption of continuity of the Fra Mauro Formation by the cover of younger Copernicus ejecta and the controversy surrounding the interpretation of individual Apollo 14 breccia samples (e.g. Stöffler et al. 1989; Stöffler 1989; Stadermann et al. 1991) led to alternative suggestions that not all samples from this landing site represent the Fra Mauro Formation or originate from the Imbrium basin. The matter is complicated further by the possibility that pre-Imbrian material local to the Apollo 14 site may have been mixed with the Imbrium ejecta during its deposition (Head and Hawke 1975; Hawke and Head 1977; Stöffler 1989).

Attempts to determine the age of the Imbrium impact have included studies of the Rb-Sr and ^{40}Ar-^{39}Ar systems of Apollo 12, 15 and 16 samples and initially led to an estimate of 3900-3850 Ma (e.g. Papanastassiou and Wasserburg 1971; York et al. 1972; Wilhelms et al. 1987; Stöffler et al. 2006). Subsequent work linked the Apollo 15 KREEP basalts (characterised by high concentrations of K, Rare Earth Elements and P) with the impact and, based on the Rb-Sr and ^{40}Ar-^{39}Ar ages of these samples, also suggested that the impact occurred at approximately 3840 Ma (Dalrymple and Ryder 1991; 1993; Ryder 1994). A counter argument focused on Rb-Sr and ^{40}Ar-^{39}Ar ages of impact melt breccias from the Apollo 14 and 16 landing sites, and indicated a younger age of 3750 Ma (Deutsch and Stöffler 1987; Stadermann et al. 1991).

Several more recent attempts to determine the ages of lunar breccia samples proposed to originate from the Imbrium basin have utilised U-Pb systematics of a number of U-bearing accessory minerals. A ^{207}Pb/^{206}Pb age of 3909±13 Ma (2σ) was obtained for zircon grains in the crystalline impact melt lithology of the lunar meteorite SaU 169 by Gnos et al. (2004). The composition of the meteorite,

particularly its enrichment in KREEP components, when compared with Apollo samples and remote sensing data led to the meteorite being linked with the nearside Procellarum KREEP terrane (PKT; Jolliff et al. 2000; Fig. 1), and more specifically with the Imbrium impact ejecta deposit. A separate study by Liu et al. (2012) analysed additional zircon from SaU 169, and compared those with zircon from compositionally similar high-Th impact melt breccias (IMB) from the Apollo 12 landing site. The U-Pb ages obtained for these samples (SaU 169 = 3920±12 Ma and Apollo 12 IMB = 3914±7 Ma; both errors are 2σ) are in good agreement with the Gnos et al. (2004) study and reinforce the argument for an older age of the Imbrium impact. It is also notable that suggested revisions of the decay constants and monitor ages used to calculate Rb-Sr and ^{40}Ar-^{39}Ar ages would make the earlier Imbrium age estimates within error of this older age (Liu et al. 2012). In addition to these studies, Seddio et al. (2013; 2014) obtained crystallisation ages of 3.9-3.8 Ga for several accessory phases in two Apollo 12 granite fragments, which they interpret as possibly crystallising from KREEP-rich melts generated by the Imbrium impact.

The U-Pb isotope system is known to be significantly more susceptible to resetting in Ca-phosphates than in zircon, with a closure temperature of the former typically estimated at 450-500 °C (Cherniak et al. 1991; Krogstad and Walker 1994; Chamberlain and Bowring 2001). While this relatively low-temperature resetting limits the ability of U-Pb system to ascertain the original crystallisation ages of these phases, it enhances their ability to date significant impact events.

A previous attempt to date apatites from the Apollo 14 sample suite yielded an overall age of 3926±3 Ma (2σ) for the combined set of data from four Apollo 14 breccias (Nemchin et al. 2009). However, the precision of these data for individual samples was significantly lower (uncertainties between 20-30 Ma). More recent work by Merle et al. (2014) has achieved significantly better precision and indicated an older U-Pb age of 3938±4 Ma (2σ) from Ca-phosphates in the impact breccia sample 14311. A key point highlighted in the Merle et al. (2014) study was a revised cleaning procedure, which was considered to have been more effective at removing surface contamination and, consequently, led to significantly higher ^{206}Pb/^{204}Pb ratios (i.e. lower contamination from terrestrial Pb) than those obtained by Nemchin et al. (2009). In the present study we aim to provide data with a similar precision level for an additional four Apollo 14 samples and use this improved precision to further investigate the homogeneity (or lack thereof) of the Apollo 14 breccias.

2. Analysed Samples

U-Pb Secondary Ion Mass Spectrometry (SIMS) analyses were made on Ca-phosphates from four Apollo 14 impact melt breccia samples; 14305, 14306, 14314 and 14321. The locations from which the samples were collected are indicated in Fig. 2.

Previous petrographic studies of these four breccias have illustrated the complex nature of the samples with a range of basaltic and plutonic clasts being identified in addition to the impact lithologies (e.g. Warren and Wasson 1980; Warren et al. 1983; Shervais et al. 1983; Taylor et al. 1983). All the samples have been described as crystalline matrix breccias (e.g. Knoll 1981), and the sections of 14306 and 14314 where Ca-phosphates have been dated in this study do indeed show matrices of crystalline material. The matrix is composed primarily of subhedral to anhedral equant plagioclase and pyroxene grains (typically 5-20 μm in size) with curved grain boundaries (Fig. A.1), and is similar to the granulitic impactite textures described for samples from Apollo 15, 16 and 17, and the lunar meteorite NWA 3163 (Warner et al. 1977; Lindstrom and Lindstrom 1986; Cushing et al. 1999; Hudgins et al. 2011). However, the investigated sections of 14305 and 14321 are more lithologically complex, and appear to have more fragmental and less coherent matrices (Fig. A.1). The crystalline impactite material is still the most abundant lithology in these samples, but instead occurs as clasts within the fragmental matrices of the samples. The matrices themselves also appear to consist mostly of smaller fragments (approximately 10-100 μm in size) of similar crystalline material. Large (up to ~3 mm) clasts of subophitic basalt are also present in both samples but are more common in 14321.

Particular attention has been paid to 14321 as a part of the chronological work on Apollo 14 samples (e.g. Duncan et al. 1975a; Duncan et al. 1975b; Grieve et al. 1975; Lindstrom et al. 1984), with a range of different ages (3.83-4.37 Ga) being determined for clasts and minerals in this breccia (Turner et al. 1971; York et al. 1972; Dasch et al. 1987; Meyer et al. 1996; Nemchin et al. 2006). A similarly wide range of ages (3.83-4.35 Ga) was obtained for the components of 14305 (Taylor et al. 1983; Shih et al. 1986; Nemchin et al. 2008). It should be noted that the youngest of the ages for these samples were determined by the ^{40}Ar-^{39}Ar and Rb-Sr methods, and do not reflect the revised decay constants discussed above.

Meyer et al. (1996) and Nemchin et al. (2008) obtained ^{207}Pb-^{206}Pb ages for zircons in eight Apollo 14 breccias, including 14305, 14306 and 14321. These studies yielded an array of ages between ~3.90-4.35 Ga. The zircon ages in these breccias have been interpreted as representing magmatic events, rather than impact events and breccia formation ages (Meyer et al. 1996; Nemchin et al. 2008), with the exception of particular zircon grains where their petrologic setting and textural features can be linked to impact processes (Grange et al. 2013). Combining the datasets of zircons in Apollo 14 breccias, Nemchin et al. (2008) identified several apparent spikes in the zircon ages, which they attributed to periods of KREEP magmatism at approximately 4.00, 4.20 and 4.35 Ga.

The cosmic ray exposure (CRE) ages obtained for 14306 and 14321 suggest that both samples were excavated in the impact that formed Cone Crater at approximately 25 Ma (Burnett et al. 1972; Crozaz et al. 1972; Drozd et al. 1974; Arvidson et al. 1975). Despite having a similar CRE age (27.6±1.5 Ma), 14305 has previously been interpreted as having been excavated by a separate impact due to the

distance between the sampling location and Cone Crater (>1000 m; Eugster et al. 1984). As yet, no CRE age has been reported for 14314. The 14311 sample studied by Merle et al. (2014), has a significantly older CRE age of 661±51 Ma (Drozd et al. 1974).

3. Analytical Methods

The sample thin sections were cleaned with distilled water and ethanol before being carbon coated. Back scattered electron (BSE) and elemental maps of the samples were made with a Quanta 650 FEGSEM and accompanying Oxford Instruments Energy Dispersive Spectroscopy (EDS) detector at Stockholm University. The element maps were then used to identify Ca-phosphate phases for SIMS analyses. Further, semi-quantitative analysis of the phosphate grains was performed with the same SEM setup to determine the chemical composition of the phosphates and distinguish between apatite and merrillite. The SEM maps and analyses of the samples were acquired with an accelerating voltage of 20 kV at a working distance of 10 mm.

Following the SEM documentation of the samples and prior to the SIMS analyses, a thorough cleaning process was applied (similar to that outlined by Merle et al. 2014) in order to remove surficial contamination from terrestrial Pb, which can be introduced during the sample preparation, particularly during polishing. This involved cleaning the samples with distilled water and ethanol in an ultrasonic bath before gold coating them. The Ca-phosphate U-Pb systems were analysed using a CAMECA IMS 1280 ion microprobe at the NordSIMS facility at the Swedish Museum of Natural History, Stockholm, using a methodology similar to that outlined in previous studies (e.g. Nemchin et al. 2009). The measurements were made with a primary beam current between 1-3 nA and a spot size of 5-10 µm. For each area analysed, a 15-20 µm area was pre-sputtered for 80 seconds to remove the Au coating and minimise surface contamination. Sample data were calibrated against measurements made on the BR2 2058 Ma apatite standard with a uranium concentration of 67 ppm and $^{206}Pb/^{204}Pb > 500$ (Grange et al. 2009). Data were then processed using in-house SIMS data reduction spreadsheets and the Excel add-in Isoplot (version 4.15; Ludwig 2008). The Pb isotopic compositions (particularly the $^{204}Pb/^{206}Pb$ and $^{207}Pb/^{206}Pb$ ratios) of the phases reflect the very radiogenic nature of the grains analysed, with minimal evidence of an initial lunar Pb component (Fig. 3). However, the effect of terrestrial common Pb contamination is observable in the data (primarily in sample 14305; Fig. 3b). The data were, therefore, corrected for common Pb using the model of Stacey and Kramers (1975) and their values for present-day terrestrial Pb isotopic ratios. Calculation of the U-Pb ages of the samples requires a correction for matrix effects using independently characterised reference materials. This correction inevitably leads to extra uncertainty associated with minor differences in mineral chemistry and crystal structure (between apatites and merrillites; e.g. Jolliff et al. 2006), as well as variations in instrumental conditions during the analysis of standards and unknown samples. Although some of these effects will be less significant in the apatite analyses, the lack of a suitable merrillite standard means that the

merrillite analyses were necessarily corrected with the BR2 apatite standard and may, therefore, be particularly susceptible to such matrix effects. Consequently, $^{207}Pb/^{206}Pb$ ratios, which are less affected than the inter-element U-Pb ratios by such sample-standard mismatches, are considered to give the best estimate of the sample ages and are the primary focus of the following discussion. Individual analyses discussed in the following sections have been stated with 2σ errors. All of the average ages obtained from our data are calculated at the 95% confidence limit. Calculated average age values were only accepted if they had a probability of fit (P) greater than 0.05.

Further, post-SIMS, SEM images were acquired of the analysed phases to assess the exact locations of the SIMS analyses. These images were useful for identifying instances where, for example, the analyses might have hit small fractures, not visible in the SIMS reflected light camera, or where the SIMS pits overlapped mineral grain boundaries. Such analyses were eliminated from the final dataset.

4. Results

A significant number of the phosphates yield slightly reversely discordant U-Pb data (Fig. 4), which we interpret to be the result of minor matrix differences (merrillite vs. apatite) and surface imperfections in the thin sections. Out of the 16 apatite analyses (where matrix effects should be less problematic), five analyses are not concordant within error, which we attribute to the proximity of the analyses to the nearby imperfections in the sample surface, such as cracks and void spaces. As a result, calculation of concordia ages (sensu Ludwig 1998) is impossible, and the ages presented in the following discussion are based on the $^{207}Pb/^{206}Pb$ ages. The phosphates from three of the studied samples (14305,103; 14306,150; 14314,13) yielded average $^{207}Pb/^{206}Pb$ ages of 3926±4 (MSWD = 1.0, P = 0.43), 3926±6 (MSWD = 0.56, P = 0.85) and 3929±4 Ma (MSWD = 1.4, P = 0.12) respectively (Table 1; Fig. 5). Three merrillite grains (grains 51-53; Fig. 6e) within a single lithic clast in 14305 have a weighted average $^{207}Pb/^{206}Pb$ age of 3946±15 Ma (MSWD = 0.19, P = 0.83), which is significantly older than the majority of the ages obtained for that sample (3924±4 Ma; Fig. 5; Table B.1). A single merrillite grain (grain 21; Fig. 6f) in 14314,13 also appears to be older than the rest of the phosphates analysed in that sample, with a mean $^{207}Pb/^{206}Pb$ age of 3958±19 Ma, based on five analyses (MSWD = 1.4, P = 0.23). One outlier from the main group is identified in the 14306,150 data.

When compared with the other three samples studied, the phosphates in 14321,134 yield a significantly older $^{207}Pb/^{206}Pb$ age of 3943±5 Ma (MSWD = 1.3, P = 0.27; Fig. 5). This age is based on six analyses: four of which come from a single apatite grain and yield $^{207}Pb/^{206}Pb$ ages between 3940±6 Ma to 3945±7 Ma (Table B.1); two analyses were made in a separate merrillite grain, and have larger errors on their $^{207}Pb/^{206}Pb$ ages (±23-30 Ma) but are still within error of the first grain (Fig. 5). A seventh analysis was made in a second apatite grain (Grain 26), for which a younger $^{207}Pb/^{206}Pb$ age was obtained (3903±22 Ma; Fig. 5). Based on this measurement alone, it is unclear whether this

younger age is an analytical artefact, or whether the grain may be part of a younger lithology in the breccia. Inaccuracy in the $^{207}Pb/^{206}Pb$ ages can be caused by correction for inappropriate common Pb (see Section 5.1), but in the case of this grain, the $^{206}Pb/^{204}Pb$ ratios (Table B.1) indicate low amounts of common Pb. The location of the grain, adjacent to a relatively large void space, gives further reason to suspect that the young age may indeed be an analytical artefact (Fig. 6i).

There are no systematic differences observed in the $^{207}Pb/^{206}Pb$ ages between those that were obtained from apatites versus those obtained from merrillite. Although the merrillite analyses appear to be slightly more reversely discordant than the apatite analyses (Figs. 4 and A.2), the relative lack of apatites analysed makes it hard to confirm the consistency of this observation. Nevertheless, this observation further justifies the decision to focus primarily on the $^{207}Pb/^{206}Pb$ ages rather than the U-Pb ages. Additionally, the U and Th concentrations of the different Ca-phosphate phases appear to be distinct (Fig. A.3).

5. Discussion

5.1. Ages of the Apollo 14 impact breccias

5.1.1. Two age groups of Apollo 14 phosphates

The ages of the analysed samples fall into two main groups: (1) the majority of the grains from 14305, 14306 and 14314, which have a mean $^{207}Pb/^{206}Pb$ age of 3927±2 Ma (MSWD = 1.07, P = 0.33; Fig. 7a); and (2) two of the 14321 grains and the older grains in 14305 and 14314, which have a mean $^{207}Pb/^{206}Pb$ age of 3944±4 Ma (MSWD = 1.5, P = 0.12; Table 1; Fig. 7b). This younger age is consistent with the 3926±3 Ma apatite Pb-Pb isochron age determined by Nemchin et al. (2009) for Apollo 14 breccias. It is also notable that the older age is consistent with the 3938±4 Ma age reported by Merle et al. (2014) for the Apollo 14 breccia 14311. Combining the 14311 $^{207}Pb/^{206}Pb$ phosphate ages with the older ages in this study leads to an average age of 3941±3 (MSWD = 1.7, P = 0.01; Fig. 7d).

5.1.2. Possible effects of initial lunar Pb and/or incomplete Pb loss during an impact

The $^{207}Pb/^{206}Pb$ ages are sensitive to mixing with both terrestrial common Pb and initial lunar Pb incorporated during the crystallisation of the phosphates. As was discussed in Section 3, the Pb isotopic compositions of the grains primarily indicate the effects of terrestrial contamination, for which the data have been corrected. This is particularly evident in the trend of $^{204}Pb/^{206}Pb$ and $^{207}Pb/^{206}Pb$ ratios towards modern terrestrial Pb compositions (Fig. 3). However, the presence of even ~1% of initial lunar Pb unsupported by in situ decay of U would have the effect of generating $^{207}Pb/^{206}Pb$ ages artificially older by about 10 Ma and, therefore, presents one possible explanation for the older set of ages in this study. Nevertheless, this lunar initial Pb is unlikely to have a significant

influence on the presented set of data as illustrated here using an example of four analyses within a single phosphate (grain 1) in 14321, which have the lowest $^{204}Pb/^{206}Pb$ ratios of all the analyses in this study (Fig. 3; Table B.1). The analyses in this grain also yielded some of the older ages in this study. If terrestrial contamination is the only Pb component added to the in situ accumulated radiogenic Pb, the correction of data obtained for this grain results in a smaller spread of ages (as indicated by the blue rectangle in Fig. 3c). If the range of $^{204}Pb/^{206}Pb$ ratios between these four analyses (particularly analyses 1-1 and 1-2) is due solely to the presence of lunar initial Pb, correcting for this would result in a spread of ages for this grain from about 3937 to about 3912 Ma (indicated by the orange rectangle in Fig. 3c). These ages are younger than the 3943±5 Ma average age for the 14321 sample determined above, but have an excess scatter, hence, lunar initial Pb cannot be the only component added to the in situ accumulated Pb, and terrestrial contamination must be a significant proportion of this component. An intermediate case between these two extremes is the only means of making 14321 ages significantly younger than the age stated above. While an explicit test of this intermediate case is impossible due to the lack of information about the proportion of mixing between terrestrial and possible lunar initial Pb, some constraints can be placed using the existing data. In the $^{207}Pb/^{206}Pb$ vs. $^{204}Pb/^{206}Pb$ coordinate space, mixing relationships between pure lunar initial Pb and radiogenic Pb accumulated in the grains (as a result of U decay after the U-Pb system became closed for Pb diffusion) are defined by a straight line that has to pass left of the analysis with the lowest $^{204}Pb/^{206}Pb$ or through this analytical point as a limiting case (i.e. analysis 1-1 in grain 1 of 14321; Figs. 3c and 3d). The close proximity of this analysis to the vertical axis restricts the potential reduction of observed age by correcting for lunar initial Pb to a few million years, i.e. not sufficient to make 14321 similar to the rest of the analysed samples. Correcting all the analyses of this grain for terrestrial Pb contributions will result in the projection of all analytical points to a single point on the lunar initial Pb-in situ Pb mixing line (Fig. 3d). This would imply similar mixing fractions of lunar initial and in situ radiogenic Pb (Pb_i and Pb_r in Fig. 3d) for all analyses in grain 1. As the amount of in situ Pb is a function of U concentration, which varies significantly between the analyses (Table B.1), then the fraction of the lunar initial Pb component will also be correlated with the amount of U content incorporated into different parts of a single phosphate grain. While such a correlation is not completely impossible, it is highly improbable as incorporation of U and initial lunar Pb into phosphates is likely to occur at different times and result from completely different geochemical and/or physical processes – i.e. with U being incorporated into the grains during crystallisation, while the initial lunar Pb would have been introduced and mixed with the Pb in the phosphate grains during later impact events where the system is opened for Pb mobility. Consequently it is highly likely that the observed younger and older groups of phosphate grains are not a result of inappropriate correction for unsupported Pb. In 14305 and 14314, the consistency of the $^{204}Pb/^{206}Pb$ and $^{207}Pb/^{206}Pb$ ratios between the younger and older grains, and the lack of any significant deviation in the older grains towards a potential lunar initial Pb composition, also argue against the effect of initial lunar Pb (Fig. 3). Furthermore, the

consistency of the second age between 14321, the older grains in 14305 and 14314, and the 14311 sample analysed by Merle et al. (2014), strengthens the case that the 3940 Ma age is genuine.

It is also assumed that the U-Pb system within the phosphates is perfectly reset during impact (i.e. the in situ accumulated Pb is completely lost). If this is not the case, any remaining Pb will also lead to artificially older $^{207}Pb/^{206}Pb$ ages. Although it is difficult to completely exclude this possibility, the recurrence of the same ~3940 Ma age in several samples from the Apollo 14 landing site suggests that the older age is genuine. In theory, the distribution of ages in a set of analyses can provide an additional check; where a perfect Gaussian distribution would be expected in completely reset grains, with the width of the distribution determined purely by analytical scatter. Conversely, incomplete resetting will result in a smooth distribution, with a main peak close to the time of the event, but with a larger tail towards the older ages, generated by the presence of the incompletely reset phosphates. The available set of data (from this study and that of Merle et al. 2014) produce a distribution with a main maximum at about 3930 Ma and a bulge close to 3940 Ma (Fig. 8a). Plotting the younger and older grains from these datasets separately results in two bell shaped (Gaussian) distributions, indicating the absence of any additional uncertainty beyond the analytical scatter (Figs. 8b and 8c). Therefore, based on the currently available datasets in this study and that of Merle et al. (2014), we interpret the two ages as representing distinct events. Nevertheless, it will only become possible to test this interpretation thoroughly as future studies add to the database of ages in the literature for other Apollo 14 breccias, as well as breccias from other landing sites. If more analyses continued to yield the same two ages it would improve the confidence of this interpretation. However, if additional analyses resulted in a range of intermediate ages, it would become increasingly hard to separate the ages into two distinct groups. This might indicate that the statistical precision of the method (<5 Ma) has begun to exceed its limit of achievable accuracy (perhaps ~10-20 Ma), determined by factors such as the presence of grains where the U-Pb is incompletely reset. Additionally, applying a combination of dating techniques, capable of producing high precision data (such as U-Pb in phosphates and ^{40}Ar-^{39}Ar), to the same samples, can help to confirm the reliability of obtained ages.

5.1.3. Textural relationships of analysed phosphates and their ages

The younger phosphates analysed in 14305, 14306 and 14314 are typically <150 μm in size (Fig. 6a-d). Those analysed in 14306 and 14314 are located within the crystalline matrices of the samples (Fig. 6b-d). Most of the analysed phosphates in 14305 are also located in clasts of the crystalline impactite lithology that dominates the sample. The older ages, such as those from 14321, grains 51-53 of 14305, and grain 21 of 14314, typically come from larger (>150 μm) or more brecciated and deformed grains (Figs. 6c and 6e), or grains located in larger (>200 μm) mineral assemblages that do not appear to have been completely recrystallized (Figs. 6b and 6d). These are interpreted as representing older (i.e. pre-breccia formation) lithologies incorporated into the breccias. The larger size of many of these

grains (e.g. grain 21 in 14314, and grain 1 in 14321; Fig. 6f and 6g) and the location of smaller old grains within lithic clasts (e.g. grains 51-53 in 14305; Fig. 6e), may explain why the U-Pb system in them has resisted resetting by the more recent impact event. It is notable that the U and Th concentrations in these older phosphates do appear to vary from the younger grains (Fig. A.3). The exact nature of this variation is hard to determine on the basis of the current data set, but may reflect different source compositions (KREEP vs. non-KREEP?) of the older and younger material.

5.1.4. Comparison of phosphate ages with previously obtained Apollo 14 breccia ages

Comparison of the data from this study with the ^{40}Ar-^{39}Ar and Rb-Sr data present in the literature for Apollo 14 samples highlights a significant discrepancy between our average lower ^{207}Pb/^{206}Pb age of 3927±2 Ma and the commonly cited age range of 3900-3750 Ma (e.g. Papanastassiou and Wasserburg 1971; Turner et al. 1971; Stadermann et al. 1991; Stöffler et al. 2006). Recalculation of these ^{40}Ar-^{39}Ar and Rb-Sr ages, to reflect more recent decay constants and monitor ages, may improve the consistency in some cases (Liu et al. 2012). However, to more fully address this issue, we propose that the literature data be filtered according to a more stringent set of criteria prior to making any comparison. This includes the requirements that: (1) the samples are clearly linked to impact processes (e.g. impact melts and breccias); (2) ages are given with a minimum precision of ± 40 Ma (2σ); (3) the calculated weighted-mean age for ^{40}Ar-^{39}Ar datasets includes at least 3 consecutive steps comprising either more than 50% (mini-plateau, i.e. somewhat robust) or 70% (plateau, i.e. robust) of ^{39}Ar degassed (e.g. McDougal & Harrison 1999 and references therein); (4) Rb-Sr isochrons are based on more than three points; (5) only ^{40}Ar-^{39}Ar plateau ages and Rb-Sr isochron lines with a probability of fit (P) $\geq$ 0.05 are considered as statistically valid (e.g. Mahon 1996; Baksi 2007; Jourdan et al. 2009).

A full description of how these criteria were applied to each dataset can be found in the accompanying appendix text. On the basis of these criteria, none of the ^{40}Ar-^{39}Ar datasets for Apollo 14 impact melt breccias are acceptable. Application of these criteria to the available Rb-Sr datasets leads us to exclude all but two datasets for the sample 14310 (Papanastassiou and Wasserburg 1971; Mark et al. 1974) and one dataset for 14078 (McKay et al. 1978). Both of these samples have been interpreted as KREEP-rich basalts and, unlike the impact breccias, cannot be unambiguously linked with an impact event. As such, their connection with the Imbrium basin and the Fra Mauro Formation impact breccias is unclear. Furthermore, in the case of 14310, the discrepancy between the 3838±23 Ma age obtained by Papanastassiou and Wasserburg (1971) and the 3924±29 Ma age obtained from the data of Mark et al. (1974) casts doubts on the reliability of one, or both, data sets.

5.2. Stratigraphy of the Apollo 14 landing site

The thickness of the Fra Mauro Formation at the Apollo 14 site is not very well known. Early photogeologic studies of the region estimated a thickness of approximately 100-200 m (Eggleton and

Offield 1970; Wilhelms et al. 1987). Seismic studies performed by the Apollo 14 astronauts did not entirely resolve this issue but analysis of this data by Watkins and Kovach (1972) provided a lower (16 m) and upper (76 m) estimate for the thickness of the formation. In addition, the thickness of the overlying unconsolidated regolith at the landing site is estimated to be between 8.5-12 m thick (Eggleton and Offield 1970; Watkins and Kovach 1972). The emplacement of the Fra Mauro Formation would have likely resulted in the entrainment and mixing of underlying lithologies, including ejecta from older basin forming events (Oberbeck 1975; Head and Hawke, 1975). If this is the case, then a simplistic assumption would be that more of this older material would occur closer to the base of the Fra Mauro Formation. As such, higher concentrations of this material might be expected in the areas surrounding craters large enough to have excavated material from beneath the Apollo 14 regolith layer and sufficiently deep into the Fra Mauro Formation.

Cone Crater is the most obvious candidate for such a crater, and the Apollo 14 traverse into and across the continuous ejecta blanket of the crater may allow us to test this hypothesis. Assuming typical crater scaling parameters (Melosh 1989), Cone Crater would have excavated material up to a depth of approximately 30 m. Therefore, if the 16 m estimate for the thickness of the Fra Mauro Formation is correct, the Cone Crater impact would have excavated material from below the formation and the ejecta would be expected to contain a minor contribution of older material (Fig. 9). If the thickness of the Fra Mauro Formation is more similar to the 76 m estimate of Watkins and Kovach (1972), then the excavation of older material would be reliant on the presence of clasts of this material in the formation originating from the underlying lithologies (Fig. 9).

Typical models of crater ejecta distribution indicate that material excavated from deeper stratigraphic levels would be primarily situated close to the rim of the crater (Melosh 1989). The sampling location of 14321 near the rim of Cone Crater, and the older overall age of the phosphates in the sample, fits well with the hypothesis that it represents ejecta excavated from the greatest depth of Cone Crater excavation and would be the most likely to contain pre-Fra Mauro material. Although a similar argument could be put forward for 14311, the older exposure age of the sample (661 Ma; Drozd et al. 1974) indicates that it is instead the result of another crater sampling the pre-Fra Mauro lithologies beneath the Fra Mauro Formation, and its location in the Cone Crater ejecta is coincidental.

The younger ca. 3927 Ma ages of the phosphates in 14305, 14306 and 14314 are interpreted to represent the age of the Fra Mauro Formation. The smaller number of older clasts and mineral fragments in 14306 and 14314 can be explained as the samples representing material excavated from shallower depths in the Fra Mauro Formation. Equally, if 14305 was assembled in a separate impact event (Eugster et al. 1984) then this impact would also be expected not to have excavated very deeply into the Fra Mauro Formation.

5.3. Apollo 14 breccias and the wider lunar context

As discussed above, the mean $^{207}Pb/^{206}Pb$ age (3927±2 Ma) of the three younger samples (14305, 14306 and 14314) is significantly older than the age estimates of Apollo 14 samples (3750-3900 Ma) determined using the Rb-Sr and ^{40}Ar-^{39}Ar isotope systems (Stöffler et al. 2006). It is closer to more recently obtained ages of zircon grains found in Apollo 12 impact melt breccia fragments and the lunar meteorite SaU 169 (Gnos et al. 2004; Liu et al. 2012). Combining the younger Apollo 14 phosphate ages reported here with the Apollo 12 zircon ages (Liu et al. 2012) and the SaU 169 zircon ages (Gnos et al. 2004) yields a weighted average age of 3926±2 Ma (MSWD = 1.3; P = 0.051; Fig. 7c). This leads us to conclude that all three sets of ages represent the same impact event.

Given that the Apollo samples originate from the lunar regolith and do not represent samples of actual bedrock exposures, interpreting the significance of the ages (e.g. which specific impact events are recorded in a set of impact breccias) remains speculative. Nevertheless, the interpretation of the Fra Mauro Formation as Imbrium ejecta (Swann et al. 1971; 1977), and the proximity of the Apollo 12 and 14 landing sites to the Imbrium basin, make a strong case for using the most common age identified in Apollo 12 and 14 impact melt breccias as an indicator for the age of the Imbrium impact. This is particularly true in the case of ages determined for phosphate grains where the U-Pb system is known to be more susceptible to resetting than that of zircon (Cherniak et al. 1991; Krogstad and Walker 1994; Chamberlain and Bowring 2001). Attributing zircon ages to impact processes requires more systematic investigation of the petrologic and textural context to identify zircon grains that are crystallising directly from the impact melts. However, ages determined for phosphates are much more likely to represent the timing of impact events in the assumption that the strong thermal pulse associated with an impact is capable of completely resetting the U-Pb systems of the existing phosphates.

It is also hard to determine the exact source locality of a lunar meteorite, so caution must be used when linking the age of SaU 169 to the formation of the Imbrium basin. Nevertheless, the distinct KREEP signature of the sample, similar texture to the Apollo 12 impact melt breccia fragments and the identical age have all been cited as reasons to link the SaU 169 ages to the Imbrium event. Taking all of these considerations into account, we speculate that our attempt to combine the Apollo 14 younger phosphate ages and those obtained for the Apollo 12 and SaU 169 zircons is justified, and that the 3926±2 Ma age determined here for 14305, 14306, 14314, the Apollo 12 impact melt breccia fragments and SaU 169, represents the most likely candidate for the Imbrium event.

5.4. Sampling a second large impact basin?

As discussed above, the younger age of ~3926 Ma seems to be a likely candidate for the Imbrium basin forming impact. This raises an obvious question; what is the source of the older (~3940 Ma) age identified in several of the Apollo 14 breccias?

The samples used to define this older age have different CRE ages (~25 Ma for 14305 and 14321; 661±51 Ma for 14311; Burnett et al. 1972; Crozaz et al. 1972; Drozd et al. 1974), suggesting that this older material is extensive enough to have been excavated from underneath the Fra Mauro Formation by more than one crater and, therefore, may represent a second underlying continuous ejecta deposit. Two large pre-Imbrian basins (Humorum and Nubium) are immediately obvious south of the Apollo 14 landing site (Fig. 1). To check for any other possible candidate impact features that may have deposited ejecta beneath the Apollo 14 landing site, the diameters of the known Nectarian and pre-Nectarian craters and basins (Öhman et al. 2015) were used to estimate the radial extent of their continuous ejecta blankets. This was done using the equation:

$$R_{ce} = (2.3 \pm 0.5)R^{1.006} \quad [1]$$

where R_{ce} is the radius of the continuous ejecta blanket and R is the radius of the impact structure (Moore et al. 1974; Melosh 1989). It is acknowledged that this formula is not verified for very large (diameter > 426 km) impact features; however, it remains the only formula determined for calculating the continuous ejecta range. Two additional equations were used to further quantify the thickness (t) of ejecta from a given impact structure, predicted to be deposited at the Apollo 14 landing site. In the case of simple craters (i.e. those with a diameter <15 km) the following equation was used:

$$t = 0.04\ R\ (r/R)^{-3\pm0.5} \quad [2]$$

where r is the distance from the centre of the crater to the Apollo 14 landing site (Kring 1995). The ejecta thickness of complex craters and basins (i.e. with a diameter >15 km) was calculated using the relationship described by McGetchin et al. (1973):

$$t = 0.14\ R^{0.74}\ (r/R)^{-3\pm0.5} \quad [3]$$

A potentially significant source of error in these calculations is the variation in suggested basin diameters. The Humorum basin provides a good example of this, where two significantly different diameters can be found in the literature: 820 km (Wilhelms et al. 1987; Stöffler et al. 2006) and 425 km (Spudis 1993; Wieczorek and Phillips 1999). If the 425 km Humorum diameter is used in this calculation, then the continuous ejecta blanket would not reach the Apollo 14 landing site (Table B.2) according to equation *[1]*, although equation *[3]* indicates the presence of an approximately 17 m thick layer of Humorum ejecta at the landing site. The 820 km, on the other hand, would have resulted in a continuous ejecta blanket reaching the Apollo 14 landing site, and an approximate ejecta thickness of 200 m. Furthermore, it is the only Nectarian basin for which this is the case, even when taking the maximum estimate for the radial extent of the continuous ejecta. The next most likely candidate is Serenitatis which, assuming the upper estimate for basin diameter, would have deposited an approximately 80 m thick layer of ejecta at the landing site, despite equation *[1]* indicating that the continuous ejecta deposit would fall short of the Apollo 14 site by 40 km. Given that equation *[1]* has

not been verified for such large basins, we are reluctant to rule out Serenitatis on the basis of such a relatively small distance. Finally, the Nectaris basin would have deposited an approximately 40 m thick layer of ejecta at Apollo 14. Four pre-Nectarian impact structures (Fra Mauro, Nubium, Insularum and South Pole-Aitken) are calculated as having continuous ejecta blankets reaching the Apollo 14 landing site, of which, Insularum and South Pole-Aitken are amongst the oldest basins recognised on the Moon (Wilhelms et al. 1987; Stöffler et al. 2006). It is hard to reconcile the 15-20 Myr gap between the two age groups discussed in this study and an association with either Nectaris or any of the pre-Nectarian basins, as it would require an extremely large number of additional impact basins to have formed in the period between 3940-3925 Ma. The only other crater predicted as having a continuous ejecta blanket at the Apollo 14 landing site is the 320 m Triplet crater, which is superposed on and, therefore, clearly younger than the Fra Mauro Formation. As such, either the Humorum or Serenitatis basins appear to be the most likely candidates for this older age.

6. Conclusions

Three of the four samples analysed contain phosphates for which an average $^{207}Pb/^{206}Pb$ age of 3927±2 Ma is determined. When combined with the ages previously obtained for zircons in Apollo 12 impact melt breccia fragments and the lunar meteorite SaU 169 (Gnos et al. 2004; Liu et al. 2012), these data yield a weighted average age of 3926±2 Ma. This age is considered to be the most likely candidate for the Fra Mauro Formation and consequently the Imbrium impact.

An older age of 3944±4 Ma is determined for phosphate phases in the sample 14321, as well as several grains in 14305 and 14314, which is indistinguishable from the age determined by Merle et al. (2014) for phosphates in Apollo 14 breccia 14311. Based on currently available data, it is difficult to entirely rule out the possibility that the two age groups might result from the effects of partial resetting of the U-Pb system. However, the occurrence of a similar older age within multiple samples leads us to conclude that the two ages do indeed represent separate impact events. The older age is interpreted as dating impact ejecta units underlying the Fra Mauro Formation. Evaluation of likely sources for this older material leads us to speculate that this ~3940 Ma age may represent the formation of the Humorum or Serenitatis impact basins.

Although the links between these ages and particular lunar basins remain speculative, the precision of the data presented here has allowed us to begin resolving the signatures of multiple impact events in a way not possible with previous datasets (e.g. Nemchin et al. 2009). The potential identification of two large impact events within ~15 Myrs has important implications for the rate of lunar bombardment around 3.95-3.92 Ga. Future studies, providing additional age data at a similar precision level will allow us to better test the various models of meteorite bombardment in the early Solar System.

Acknowledgments

The authors thank the astronauts of Apollo 14 for risking their lives to collect the samples. Comments from Bradley Jolliff, Tsuyoshi Iizuka and one anonymous reviewer significantly improved the manuscript. This work was funded by grants from the Knut and Alice Wallenberg Foundation (2012.0097) and the Swedish Research Council (VR 621-2012-4370) to MJW and AAN. The NordSIMS facility is operated under a joint Nordic agreement; this is NordSIMS publication #428. The research has made use of NASA's Astrophysics Data System.

References

Arvidson R., Crozaz G., Drozd R. J., Hohenberg C. M. and Morgan C. J. (1975) Cosmic ray exposure ages of features and events at the Apollo landing sites. *The Moon* **13**, 259-276. http://doi.org/10.1007/BF00567518.

Baksi A. K. (2007) A quantitative tool for evaluating alteration in undisturbed rocks and minerals – I: water, chemical weathering and atmospheric argon. In *The origin of melting anomalies, plates, plumes and planetary processes* (eds. G. R. Foulger and D. M. Jurdy). Geol. Soc. Amer. Spec. Pap. **430**, pp. 285–304. http://doi.org/10.1130/2007.2430(15).

Baldwin R. B. (2006) Was there ever a Terminal Lunar Cataclysm? With lunar viscosity arguments. *Icarus*, **184**, 308-318. http://doi.org/10.1016/j.icarus.2006.05.004.

Burnett D. S., Huneke J. C., Podosek F. A., Russ G. P., Turner G. and Wasserburg G. J. (1972) The Irradiation History of Lunar Samples. *Lunar Planet. Sci. III*. Lunar Planet. Inst., Houston. pp. 105-107.

Chamberlain K. R. and Bowring S. A. (2001) Apatite-feldspar U-Pb thermochronometer: a reliable, mid-range (~450°C), diffusion-controlled system. *Chemical Geology* **172**, 173-200. http://dx.doi.org/10.1016/S0009-2541(00)00242-4.

Cherniak D. J., Lanford W. A. and Ryerson F. J. (1991) Lead diffusion in apatite and zircon using ion implantation and Rutherford Backscattering techniques. *Geochim. Cosmochim. Acta* **55**, 1663-1673. http://dx.doi.org/10.1016/0016-7037(91)90137-T.

Cohen B. A., Swindle T. D. and Kring D. A. (2000) Support for the Lunar Cataclysm Hypothesis from Lunar Meteorite Impact Melt Ages. *Science* **290**, 1754-1756. http://dx.doi.org/10.1126/science.290.5497.1754.

Crozaz G., Drozd R., Hohenberg C. M., Hoyt H. P., Ragan D., Walker R. M. and Yuhas D. (1972) Solar Flare and Galactic Cosmic Ray Studies of Apollo 14 Samples. *Lunar Planet. Sci. III*. Lunar Planet. Inst., Houston. pp. 167-169.

Cushing J. A., Taylor G. J., Norman M. D. and Keil K. (1999) The granulitic impactite suite: Impact melts and metamorphic breccias of the early lunar crust. *Meteoritics and Planetary Science* **34**, 185-195. http://dx.doi.org/10.1111/j.1945-5100.1999.tb01745.x.

Dalrymple G. B. and Ryder G. (1991) $^{40}Ar/^{39}Ar$ ages of six Apollo 15 impact melt rocks by laser step heating. *Geophys. Res. Lett.* **18**, 1163-1166. http://dx.doi.org/10.1029/91GL01143.

510 Dalrymple G. B. and Ryder G. (1993) $^{40}Ar/^{39}Ar$ age spectra of Apollo 15 impact melt rocks by laser
511 step-heating and their bearing on the history of lunar basin formation. *J. Geophys. Res.* **98**,
512 13085-13095. http://dx.doi.org/10.1029/93JE01222.

513 Dasch E. J., Shih C.-Y., Bansal B. M., Wiesmann H. and Nyquist L. E. (1987) Isotopic analysis of
514 basaltic fragments from lunar breccia 14321 - Chronology and petrogenesis of pre-Imbrium
515 mare volcanism. *Geochim. Cosmochim. Acta* **51**, 3241-3254. http://dx.doi.org/10.1016/0016-
516 7037(87)90132-3.

517 Deutsch A. and Stöffler D. (1987) Rb-Sr-analyses of Apollo 16 melt rocks and a new age estimate for
518 the Imbrium basin - Lunar basin chronology and the early heavy bombardment of the moon.
519 *Geochim. Cosmochim. Acta* **51**, 1951-1964. http://dx.doi.org/10.1016/0016-7037(87)90184-0.

520 Drozd R. J., Hohenberg C. M., Morgan C. J. and Ralston C. E. (1974) Cosmic-ray exposure history at
521 the Apollo 16 and other lunar sites - Lunar surface dynamics. *Geochim. Cosmochim. Acta* **38**,
522 1625-1642. http://dx.doi.org/10.1016/0016-7037(74)90178-1.

523 Duncan A. R., McKay S. M., Stoeser J. W., Lindstrom M. M., Lindstrom D. J., Fruchter J. S. and
524 Goles G. G. (1975a) Lunar polymict breccia 14321 - A compositional study of its principal
525 components. *Geochim. Cosmochim. Acta* **39**, 247-260. http://dx.doi.org/10.1016/0016-
526 7037(75)90194-5.

527 Duncan A. R., Grieve R. A. F. and Weill D. F. (1975b) The life and times of Big Bertha - Lunar
528 breccia 14321. *Geochim. Cosmochim. Acta* **39**, 265-273. http://dx.doi.org/10.1016/0016-
529 7037(75)90196-9.

530 Eggleton R. E. and Offield T. W. (1970) Geologic maps of the Fra Mauro region of the Moon, Apollo
531 14 pre-mission maps. *U.S. Geol. Survey Misc. Geol. Inv*. Map I-708.

532 Eugster O., Eberhardt P., Geiss J., Grogler N., Jungck M., Meier F., Morgeli M. and Niederer F.
533 (1984) Cosmic ray exposure histories of Apollo 14, Apollo 15, and Apollo 16 rocks. *Lunar*
534 *Planet. Sci. XIV*. Lunar Planet. Inst., Houston. pp. 498-512.

535 Gnos E., Hofmann B. A., Al-Kathiri A., Lorenzetti S., Eugster O., Whitehouse M. J., Villa I. M., Jull
536 A. J. T., Eikenberg J., Spettel B., Krähenbühl U., Franchi I. A. and Greenwood R. C. (2004)
537 Pinpointing the Source of a Lunar Meteorite: Implications for the Evolution of the Moon.
538 *Science* **305**, 657-660. http://dx.doi.org/10.1126/science.1099397.

539 Grange M. L., Nemchin A. A., Pidgeon R. T., Timms N., Muhling J. R. and Kennedy A. K. (2009)
540 Thermal history recorded by the Apollo 17 impact melt breccia 73217. *Geochim. Cosmochim.*
541 *Acta* **73**, 3093-3107. http://dx.doi.org/10.1016/j.gca.2009.02.032.

542 Grange M.L., Pidgeon R.T., Nemchin A.A., Timms N., Meyer C. (2013). Interpreting U–Pb data from
543 primary and secondary features in lunar zircon. *Geochim. Cosmochim. Acta* **101**, pp. 112–132
544 http://dx.doi.org/10.1016/j.gca.2012.10.013.

545 Grieve R. A., McKay G. A., Smith H. D. and Weill D. F. (1975) Lunar polymict breccia 14321 - A
546 petrographic study. *Geochim. Cosmochim. Acta* **39**, 229-245. http://dx.doi.org/10.1016/0016-
547 7037(75)90193-3.

548 Hawke B. R. and Head J. W. (1977) Pre-Imbrian history of the Fra Mauro region and Apollo 14
549 sample provenance. *Lunar Planet. Sci. VIII*. Lunar Planet. Inst., Houston. pp. 2741-2761.

550 Head J. W. and Hawke B. R. (1975) Geology of the Apollo 14 region (Fra Mauro): Stratigraphic
551 history and sample provenance. *Lunar Planet. Sci. VI*. Lunar Planet. Inst., Houston. pp. 2483-
552 2501.

553 Hudgins J. A., Kelley S. P., Korotev R. L. and Spray J. G. (2011) Mineralogy, geochemistry, and ^{40}Ar-
554 ^{39}Ar geochronology of lunar granulitic breccia Northwest Africa 3163 and paired stones:
555 Comparisons with Apollo samples. *Geochim. Cosmochim. Acta* **75**, 2865-2881.
556 http://dx.doi.org/10.1016/j.gca.2011.02.035.

557 Jolliff B. L., Gillis J. J., Haskin L. A., Korotev R. L. and Wieczorek M. A. (2000) Major lunar crustal
558 terranes: Surface expressions and crust-mantle origins. *J. Geophys. Res.* **105**, 4197-4216.
559 http://dx.doi.org/10.1029/1999JE001103.

560 Jolliff B. L., Hughes J. M., Freeman J. J. and Zeigler R. A. (2006) Crystal chemistry of lunar merrillite
561 and comparison to other meteoritic and planetary suites of whitlockite and merrillite. *American*
562 *Mineralogist* **91**, 1583-1595. http://dx.doi.org/10.2138/am.2006.2185.

563 Jourdan F., Renne P.R., Reimold W.U. (2009) An appraisal of the ages of terrestrial impact structures.
564 *Earth Planet. Sci. Lett.* **286**, 1–13. http://dx.doi.org/10.1016/j.epsl.2009.07.009.

565 Knoll H. D. (1981) Classification of the Rock Samples of the Apollo 14 Landing Site According to the
566 Recommended Nomenclature of Lunar Highland Rocks. *Lunar Planet. Sci. XII*. Lunar Planet.
567 Inst., Houston. pp. 553-555.

568 Kring D. A. (1995) The dimensions of the Chicxulub impact crater and impact melt sheet. *J. Geophys.*
569 *Res.* **100**, 16979-16986. http://dx.doi.org/10.1029/95JE01768.

570 Krogstad E. J. and Walker R. J. (1994) High closure temperatures of the U-Pb system in large apatites
571 from the Tin Mountain pegmatite, Black Hills, South Dakota, USA. *Geochim. Cosmochim.*
572 *Acta* **58**, 3845-3853. http://dx.doi.org/10.1016/0016-7037(94)90367-0.

573 Lindstrom M. M., Knapp. S. A., Shervais J. W. and Taylor L. A. (1984) Magnesian anorthosites and
574 associated troctolites and dunite in Apollo 14 breccias. *Lunar Planet. Sci. XV*. Lunar Planet.
575 Inst., Houston. pp. 41-49.

576 Lindstrom M. M. and Lindstrom D. J. (1986) Lunar granulites and their precursor anorthositic norites
577 of the early lunar crust. *J. Geophys. Res.* **91**, 263-276.
578 http://dx.doi.org/10.1029/JB091iB04p0D263.

579 Liu D., Jolliff B. L., Zeigler R. A., Korotev R. L., Wan Y., Xie H., Zhang Y., Dong C. and Wang W.
580 (2012) Comparative zircon U-Pb geochronology of impact melt breccias from Apollo 12 and
581 lunar meteorite SaU 169, and implications for the age of the Imbrium impact. *Earth Planet.*
582 *Sci. Lett.* **319**, 277-286. http://dx.doi.org/10.1016/j.epsl.2011.12.014.

583 Ludwig K. R. (1998) On the Treatment of Concordant Uranium-Lead Ages. *Geochim. Cosmochim.*
584 *Acta* **62**, 665-676. http://dx.doi.org/ 10.1016/S0016-7037(98)00059-3.

585 Ludwig K. R. (2008) User's Manual for Isoplot 3.60, A geochronological toolkit for Microsoft Excel.
586 *Berkeley Geochronological Center Special Publication* **4**, Berkeley, California: Berkeley
587 Geochronological Center.

McDougall I. and Harrison T. M. (1999) *Geochronology and thermochronology by the $^{40}Ar/^{39}Ar$ method*. Oxford Univ. press, Oxford, p. 269.

McGetchin T. R., Settle M. and Head J. W. (1973) Radial thickness variation in impact crater ejecta: Implications for lunar basin deposits. Earth Planet. Sci. Lett. 20, 226-236. http://dx.doi.org/10.1016/0012-821X(73)90162-3.

McKay G. A., Wiesmann H., Nyquist L. E., Wooden J. L. and Bansal B. M. (1978) Petrology, chemistry, and chronology of 14078: Chemical constraints on the origin of KREEP. *Lunar Planet. Sci. IX*. Lunar Planet. Inst., Houston. pp. 661-687.

Mahon K. I. (1996) The new York regression: application of an improved statistical method to geochemistry. *Int. Geol. Rev.* **38**, 293-303. http://dx.doi.org/10.1080/00206819709465336.

Marchi S., Bottke W. F., Elkins-Tanton L. T., Bierhaus M., Wuennemann K., Morbidelli A. and Kring D. A. (2014) Widespread mixing and burial of Earth's Hadean crust by asteroid impacts. *Nature* **511**, 578-582. http://dx.doi.org/10.1038/nature13539.

Mark R. K., Lee-Hu C. -N. and Wetherill G. W. (1974) Rb-Sr age of lunar igneous rocks 62295 and 14310. *Geochim. Cosmochim. Acta* **38**, 1643-1648. http://dx.doi.org/10.1016/0016-7037(74)90179-3.

Melosh H. J. (1989) *Impact Cratering: A Geologic Process*. Oxford University Press, New York.

Merle R. E., Nemchin A. A., Grange M. L., Whitehouse M. J. and Pidgeon R. T. (2014). High resolution U-Pb ages of Ca-phosphates in Apollo 14 breccias: implications for the age of the Imbrium impact. *Meteoritics and Planetary Science* **49**, 2241-2251. http://dx.doi.org/10.1111/maps.12395.

Meyer C., Williams I. S. and Compston W. (1996) Uranium-lead ages for lunar zircons: Evidence for a prolonged period of granophyre formation from 4.32 to 3.88 Ga. *Meteoritics and Planetary Science* **31**, 370-387. http://dx.doi.org/10.1111/j.1945-5100.1996.tb02075.x.

Moore H. J., Hodges C. A. and Scott D. H. (1974) Multiringed basins - Illustrated by Orientale and associated features. *Lunar Planet. Sci. V*. Lunar Planet. Inst., Houston. pp. 71-100.

Morbidelli A., Marchi S., Bottke W. F. and Kring D. A. (2012) A sawtooth-like timeline for the first billion years of lunar bombardment. *Earth Planet. Sci. Lett.* **355**, 144-151. http://dx.doi.org/10.1016/j.epsl.2012.07.037.

National Research Council (NRC) of the National Academies. (2007) *The Scientific Context for Exploration of the Moon*. National Academies Press, Washington, DC.

Nemchin A. A., Whitehouse M. J., Pidgeon R. T. and Meyer C. (2006) Oxygen isotopic signature of 4.4-3.9 Ga zircons as a monitor of differentiation processes on the Moon. *Geochim. Cosmochim. Acta* **70**, 1864-1872. http://dx.doi.org/10.1016/j.gca.2005.12.009.

Nemchin A. A., Pidgeon R. T., Whitehouse M. J., Vaughan J. P. and Meyer C. (2008) SIMS U-Pb study of zircon from Apollo 14 and 17 breccias: Implications for the evolution of lunar KREEP. *Geochim. Cosmochim. Acta* **72**, 668-689. http://dx.doi.org/10.1016/j.gca.2007.11.009.

Nemchin A. A., Pidgeon R. T., Healy D., Grange M. L., Whitehouse M. J. and Vaughan J. (2009) The comparative behavior of apatite-zircon U-Pb systems in Apollo 14 breccias: Implications for the thermal history of the Fra Mauro Formation. *Meteoritics and Planetary Science* **44**, 1717-1734. http://dx.doi.org/10.1111/j.1945-5100.2009.tb01202.x.

Oberbeck V. R. (1975) The role of ballistic erosion and sedimentation in lunar stratigraphy. *Rev. Geophysics and Space Physics* **13**, 337-362. http://dx.doi.org/10.1029/RG013i002p00337.

Öhman T., Losiak A., Kohout T., O'Sullivan K., Thaisen K. and Weider S. (2015) Impact Crater Database (third edition), Lunar and Planetary Institute, Houston, TX. http://www.lpi.usra.edu/lpi/sci_database.shtml.

Papanastassiou D. A. and Wasserburg G. J. (1971) Rb-Sr ages of igneous rocks from the Apollo 14 mission and the age of the Fra Mauro formation. *Earth Planet. Sci. Lett.* **12**, 36-48. http://dx.doi.org/10.1016/0012-821X(71)90052-5.

Ryder G. (1990) Lunar samples, lunar accretion and the early bombardment of the moon. *EOS Trans. Am. Geophys. Union* **71**, 313-323. http://dx.doi.org/10.1029/90EO00086.

Ryder G. (1994) Coincidence in Time of the Imbrium Basin Impact and Apollo 15 KREEP Volcanic Flows: The Case for Impact-Induced Melting. In *Large Meteorite Impacts and Planetary Evolution* (eds. B. O. Dressler, R. A. F. Grieve and V. L. Sharpton). *Geol. Soc. Am. Spec. Paper* **293**, 11-18.

Seddio S. M., Jolliff B. L., Korotev R. L. and Zeigler R. A. (2013) Petrology and geochemistry of lunar granite 12032,366-19 and implications for lunar granite petrogenesis. *American Mineralogist* **98**, 1697-1713. http://dx.doi.org/10.2138/am.2013.4330.

Seddio S. M., Jolliff B. L., Korotev R. L. and Carpenter P. K. (2014) Thorite in an Apollo 12 granite fragment and age determination using the electron microprobe. *Geochim. Cosmochim. Acta* **135**, 307-320. http://dx.doi.org/10.1016/j.gca.2014.03.020.

Shervais J. W., Taylor L. A. and Laul J. C. (1983) Ancient crustal components in the Fra Mauro breccias. *Lunar Planet. Sci. XIV*. Lunar Planet. Inst., Houston. pp. 177-192.

Shih C.-Y., Nyquist L. E., Bogard D. D., Bansal B. M., Wiesmann H., Johnson P., Shervais J. W. and Taylor L. A. (1986) Geochronology and Petrogenesis of Apollo 14 Very High Potassium Mare Basalts. *Lunar Planet. Sci. XVI*. Lunar Planet. Inst., Houston. pp. 214-228.

Spudis, P. D. (1993) *The Geology of Multi-Ring Impact Basins*. Cambridge University Press.

Stacey J. S. and Kramers J. D. (1975) Approximation of terrestrial lead isotope evolution by a two-stage model. *Earth Planet. Sci. Lett.* **26**, 207-221. http://dx.doi.org/10.1016/0012-821X(75)90088-6.

Stadermann F. J., Heusser E., Jessberger E. K., Lingner S. and Stöffler D. (1991) The case for a younger Imbrium basin - New ^{40}Ar-^{39}Ar ages of Apollo 14 rocks. *Geochim. Cosmochim. Acta* **55**, 2339-2349. http://dx.doi.org/10.1016/0016-7037(91)90108-H.

Stöffler, D. (1989) Brecciated nature of the Apollo 14 lunar sample suite: a review. In *Moon in Transition: Apollo 14, KREEP, and Evolved Lunar Rocks* (Eds. G. J. Taylor and P. H. Warren). Lunar Planet. Inst., Houston. pp. 138-144.

Stöffler D., Bobe K. D., Jessberger E. K., Lingner S., Palme H., Spettel B., Stadermann F. and Wänke H. (1989) Fra Mauro formation, Apollo 14. IV. Synopsis and synthesis of consortium studies. In *Moon in Transition: Apollo 14, KREEP, and Evolved Lunar Rocks* (Eds. G. J. Taylor and P. H. Warren). Lunar Planet. Inst., Houston. pp. 145-148.

Stöffler D., Ryder G., Ivanov B. A., Artemieva N. A., Cintala M. J. and Grieve R. A. F. (2006) Cratering history and lunar chronology. In *New Views of the Moon* (Eds. B: L. Jolliff, M. A. Wieczorek, C. K. Shearer and C. R. Neal). Mineralogical Society of America, Rev. Min. Geochem. **60**, Chapter 5 pp. 519-596.

Swann G. A., Trask N. J., Hait M. H. and Sutton R. L. (1971) Geologic Setting of the Apollo 14 Samples. *Science* **173**, 716-719. http://dx.doi.org/10.1126/science.173.3998.716.

Swann G. A., Bailey N. G., Batson R. M., Eggleton R. E., Hait M. H., Holt H. E., Larson K. B., Reed V. S., Schaber G. G., Sutton R. L., Trask N. J., Ulrich G. E. and Wilshire H. G. (1977) Geology of the Apollo 14 landing site in the Fra Mauro highlands. *USGS Professional Paper* **880**, p. 103.

Taylor L. A., Shervais J. W., Hunter R. H., Shih C.-Y., Bansal B. M., Wooden J., Nyquist L. E. and Laul L. C. (1983) Pre-4.2 AE mare-basalt volcanism in the lunar highlands. *Earth Planet. Sci. Lett.* **66**, 33-47. http://dx.doi.org/10.1016/0012-821X(83)90124-3.

Tera F., Papanastassiou D. A. and Wasserburg G. J. (1974) Isotopic evidence for a terminal lunar cataclysm. *Earth Planet. Sci. Lett.* **22**, 1-21. http://dx.doi.org/10.1016/0012-821X(74)90059-4.

Turner G., Huneke J. C., Podosek F. A. and Wasserburg G. J. (1971) ^{40}Ar-^{39}Ar ages and cosmic ray exposure ages of Apollo 14 samples. *Earth Planet. Sci. Lett.* **12**, 19-35. http://dx.doi.org/10.1016/0012-821X(71)90051-3.

Turner G., Cadogan P. H. and Yonge C. J. (1973) Argon selenochronology. *Lunar Planet. Sci. IV*. Lunar Planet. Inst., Houston. pp. 1889-1914.

Warner J. L., Phinney W. C., Bickel C. E. and Simonds C. H. (1977) Feldspathic granulitic impactites and pre-final bombardment lunar evolution. *Lunar Planet. Sci. VII*. Lunar Planet. Inst., Houston. pp. 2051-2066.

Warren P. H., Taylor G. J., Keil K., Kallemeyn G. W., Shirley D. N. and Wasson J. T. (1983) Seventh Foray - Whitlockite-rich lithologies, a diopside-bearing troctolitic anorthosite, ferroan anorthosites, and KREEP. *Lunar Planet. Sci. XIV*. Lunar Planet. Inst., Houston. pp. 151-164.

Warren P. H. and Wasson J. T. (1980) Further foraging for pristine nonmare rocks - Correlations between geochemistry and longitude. *Lunar Planet. Sci. XI*. Lunar Planet. Inst., Houston. pp. 431-470.

Watkins J. S. and Kovach R. L. (1972) Apollo 14 Active Seismic Experiment. *Science* **175**, 1244-1245. http://dx.doi.org/10.1126/science.175.4027.1244.

Wetherill G. W. (1981) Nature and origin of basin-forming projectiles. In *Multi-ring basins: Formation and Evolution* (Eds. R. B. Merill and P. H. Schultz). Pergamon Press, New York. pp. 1-18.

Wieczorek M. A. and Phillips R. J. (1999) Lunar Multiring Basins and the Cratering Process. *Icarus* **139**, 246-259. http://dx.doi.org/10.1006/icar.1999.6102.

Wilhelms D. E., McCauley J. F. and Trask N. J. (1987) The Geologic History of the Moon. *USGS Professional Paper* **1348**.

York D., Kenyon W. J. and Doyle R. J. (1972) ^{40}Ar-^{39}Ar ages of Apollo 14 and 15 samples. *Lunar Planet. Sci. III*. Lunar Planet. Inst., Houston. pp. 1613-1622.

709 Figures and Tables

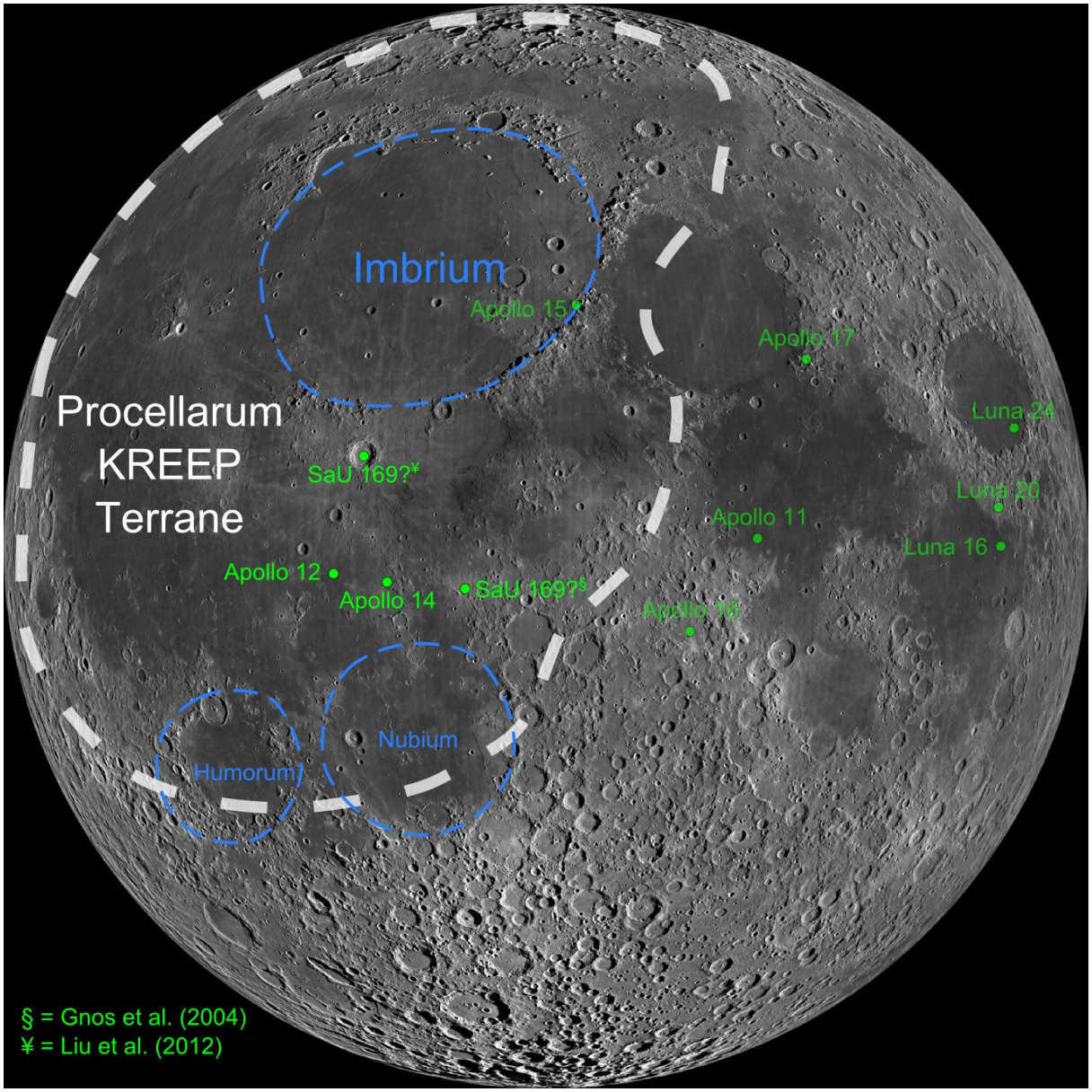

710

711 Figure 1. – Locations of lunar sample return missions and the two proposed source locations of lunar
712 meteorite SaU 169 (Gnos et al. 2004; Liu et al. 2012), with respect to the Imbrium basin. Also
713 indicated are the Nectarian and pre-Nectarian basins, Humorum and Nubium. Note, the dashed basin
714 outlines are indicated only for clarity and are approximate (i.e. they do not represent actual proposed
715 basin diameters). Also indicated (dashed white outline) is the approximate location of the Procellarum
716 KREEP Terrane, as identified by Jolliff et al. (2000). Background image is the Lunar Reconnaissance
717 Orbiter Wide Angle Camera mosaic of the lunar nearside (NASA/GSFC/Arizona State University).

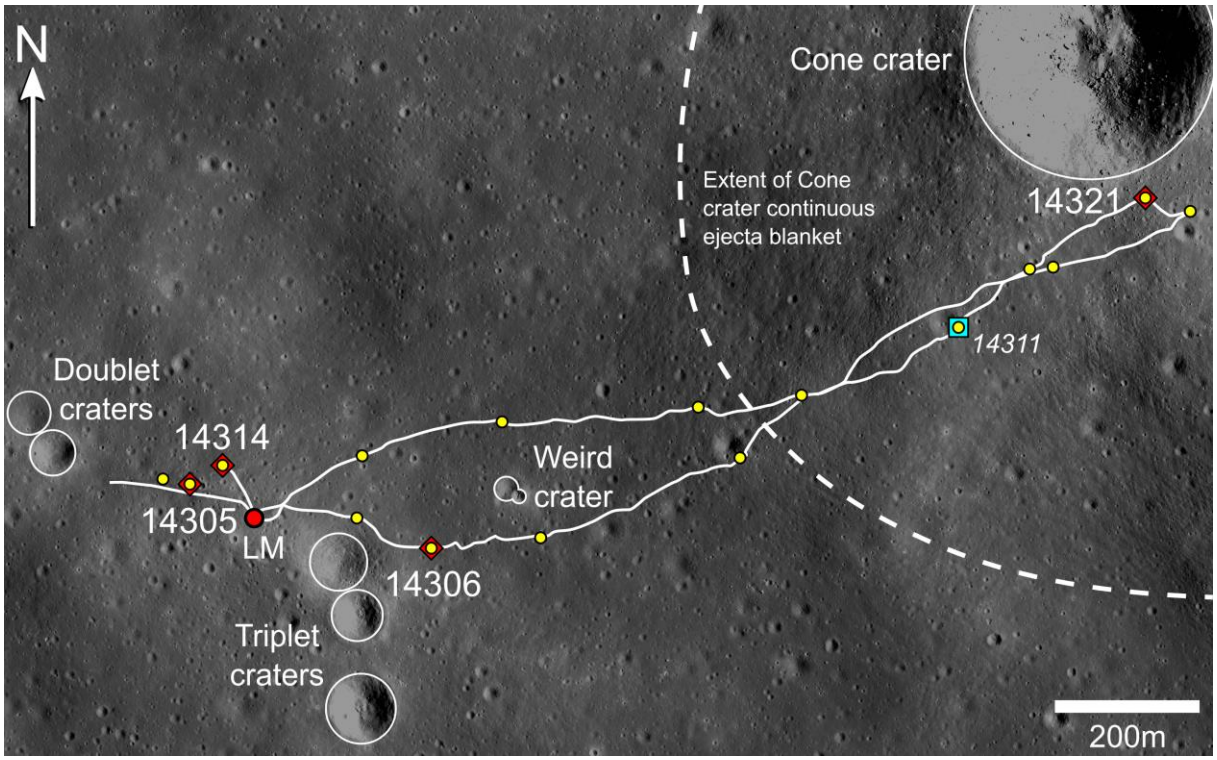

Figure 2. – Map of the Apollo 14 landing site displaying the locations from which the samples in this study were collected (red diamonds). Also shown is the collection location of sample 14311 (blue square), studied by Merle et al. (2014). The lunar module (LM) location, sample collection locations (yellow dots), EVA tracks (solid white lines), and Cone Crater continuous ejecta outline were based on maps produced by Swann et al. (1971) and Stöffler (1989). Background image is from the Lunar Reconnaissance Orbiter Narrow Angle Camera frame M129404545 (NASA/GSFC/Arizona State University).

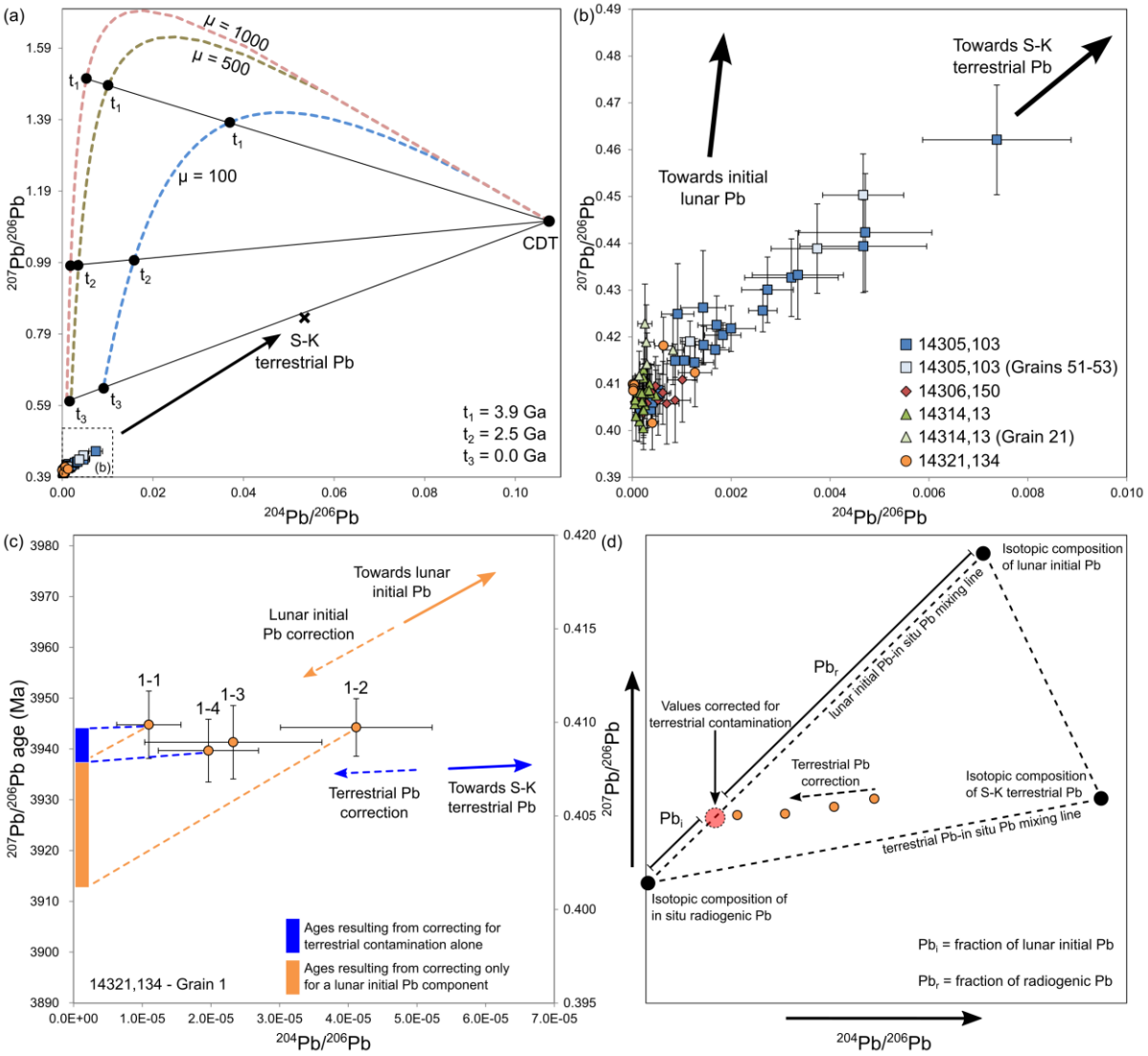

Figure 3. – (a) and (b) $^{207}Pb/^{206}Pb$ vs. $^{204}Pb/^{206}Pb$ compositions of the Apollo 14 phosphates analysed in this study (prior to correction for common terrestrial Pb) compared with the composition of common terrestrial Pb (S-K terrestrial Pb; Stacey and Kramers 1975). Within the error of these measurements, the main trend in the data is towards the S-K terrestrial Pb values, with little evidence of an initial lunar Pb component. Also indicated in (a) are several growth curves for the composition of initial lunar Pb originating from Canyon Diablo Troilite (CDT) composition. These curves assume a range of potential lunar μ ($^{238}U/^{204}Pb$) values, a formation age of ~4.5 Ga for the Moon and a simple single stage model of lunar Pb isotopic evolution. The intercept between the isochrons marked and the growth curves indicate the isotopic composition of initial lunar Pb at three arbitrary times. (c) $^{207}Pb/^{206}Pb$ age (Ma) vs. $^{204}Pb/^{206}Pb$ compositions determined from four analyses of Grain one in 14321,134. The solid arrows indicate the directions towards common terrestrial Pb and a proposed composition for initial lunar Pb, assuming a value for lunar μ of 1000, with the lunar Pb isotopic compositions originating from Canyon Diablo Troilite values at ~4.5 Ga. The dashed arrows, therefore, indicate the effects of correcting the analyses for components of terrestrial and lunar initial

Pb. (d) Schematic diagram illustrating the mixing trends between the three potential Pb components in the phosphates.

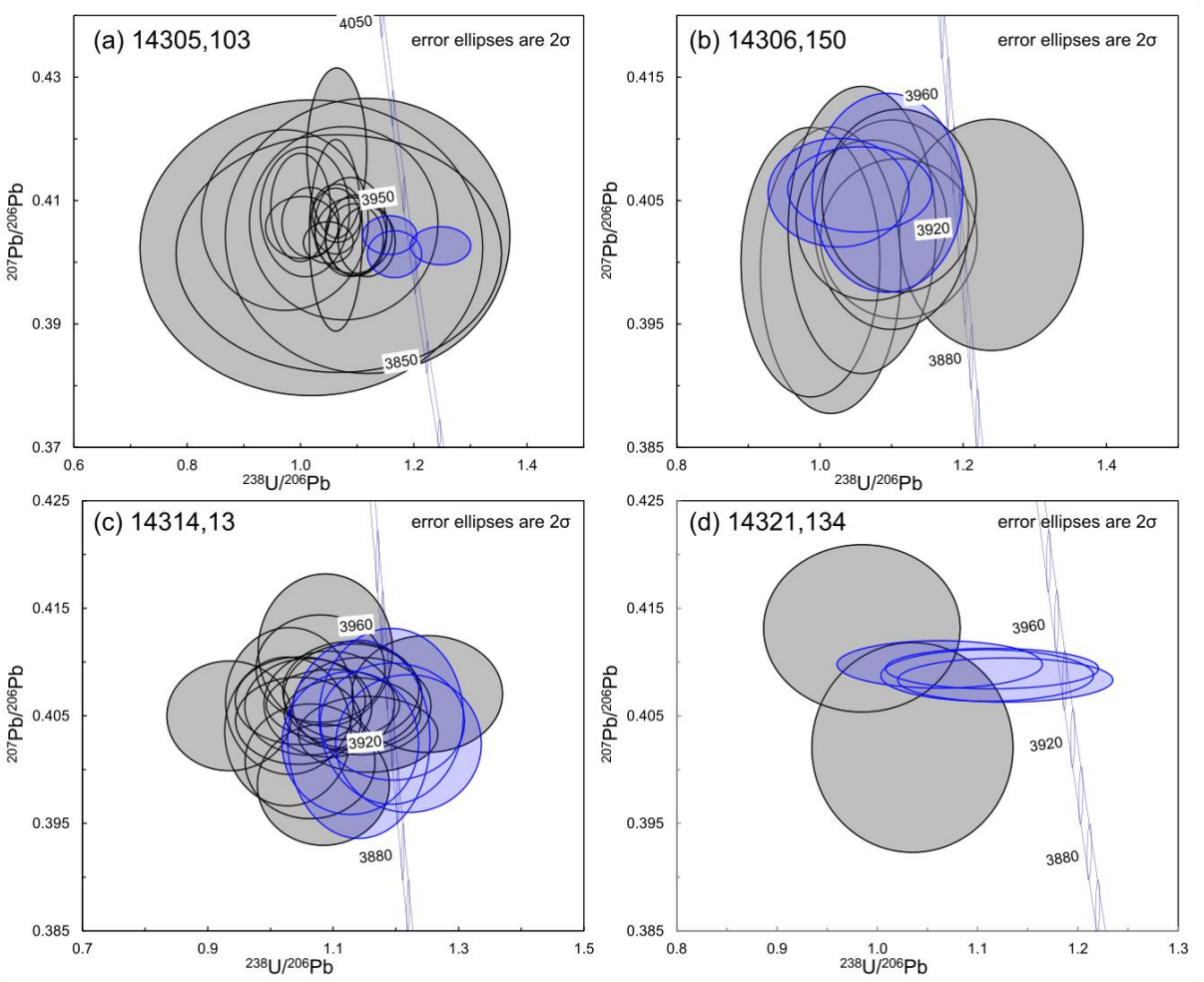

Figure 4. – Tera-Wasserburg concordia diagrams for the phosphates analysed in 14305,103; 14306,150; 14314,13; and 14321,134, with the apatite (blue) and merrillite (grey) phases highlighted. Conventional U-Pb concordia diagrams are presented in the Electronic Appendix (Fig. A.2).

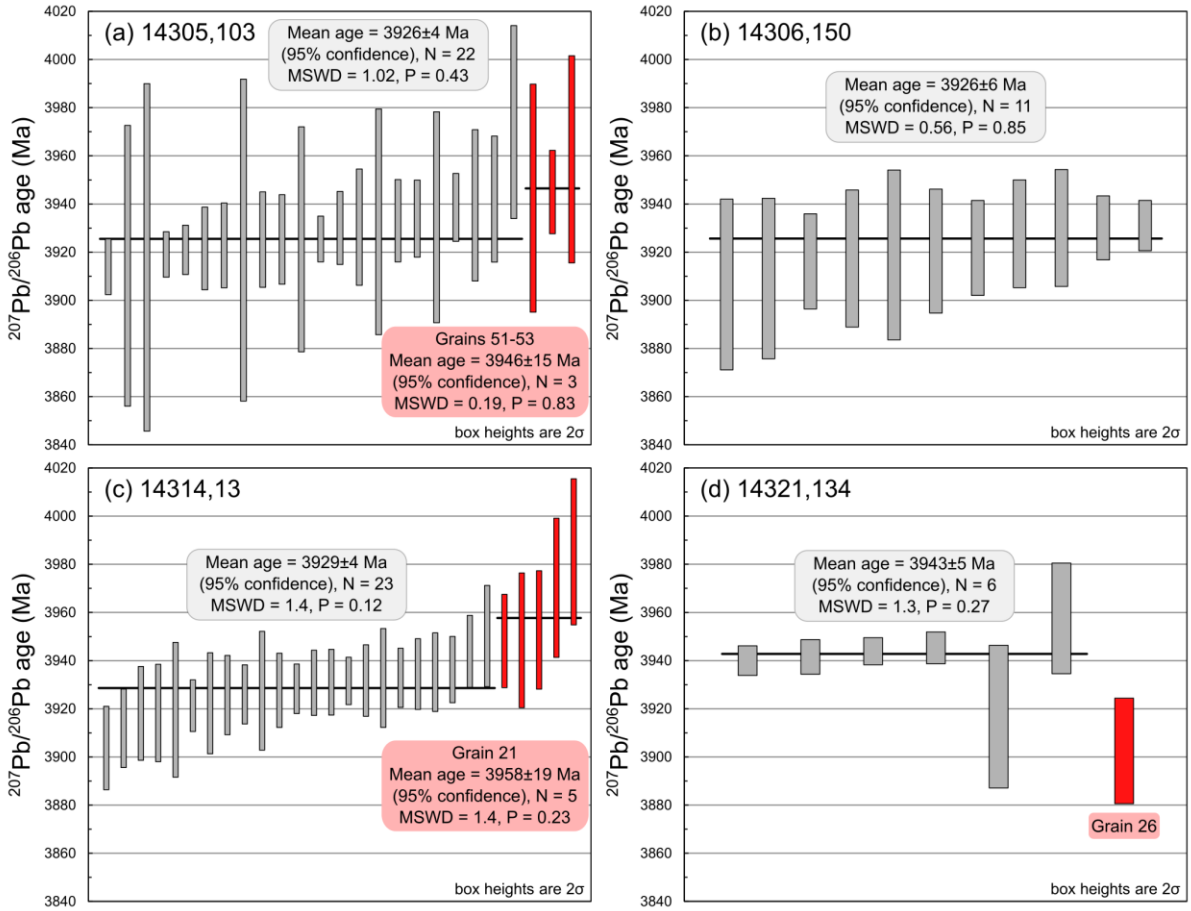

Figure 5. – The $^{207}Pb/^{206}Pb$ ages of the phosphates analysed in 14305,103; 14306,150; 14314,13; and 14321,134.

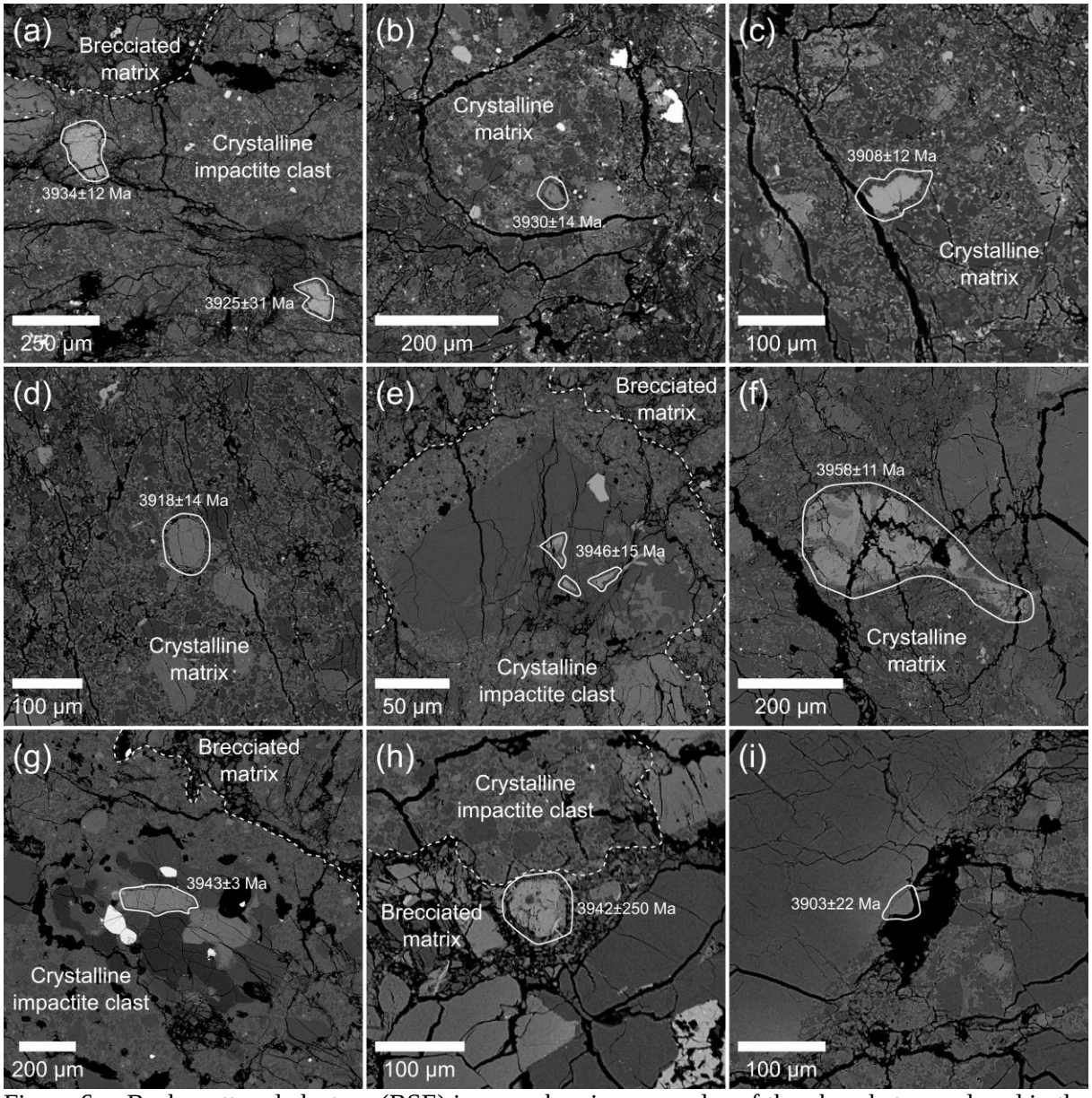

Figure 6. – Back scattered electron (BSE) images showing examples of the phosphates analysed in the four samples. The analysed grains are all outlined with solid white lines. Dashed white lines indicate the edges of clasts in the breccias. Grains 67 and 68 in 14305 (a); grain 48 in 14306 (b); and grains 27 (c) and 28 (d) in 14314,13, are typical of the types of phosphates analysed in the three younger samples. Grains 51-53 in 14305,103 (e) all occur as merrillite inclusions within a plagioclase dominated clast in a larger crystalline impactite parent clast. Grain 21 in 14314,13 (f) is a merrillite that shows more evidence of having been deformed by impact processing than most of the grains analysed. In 14321,134: grain 1 (g) is an apatite forming part of a larger mineral assemblage in an impact melt clast; grain 2 (h) occurs as a single merrillite grain in the brecciated matrix; grain 26 (i) is an apatite on the edge of a void space in a crystalline impactite clast. The average $^{207}Pb/^{206}Pb$ ages of each grain have been also indicated (errors are stated at the 95% confidence level).

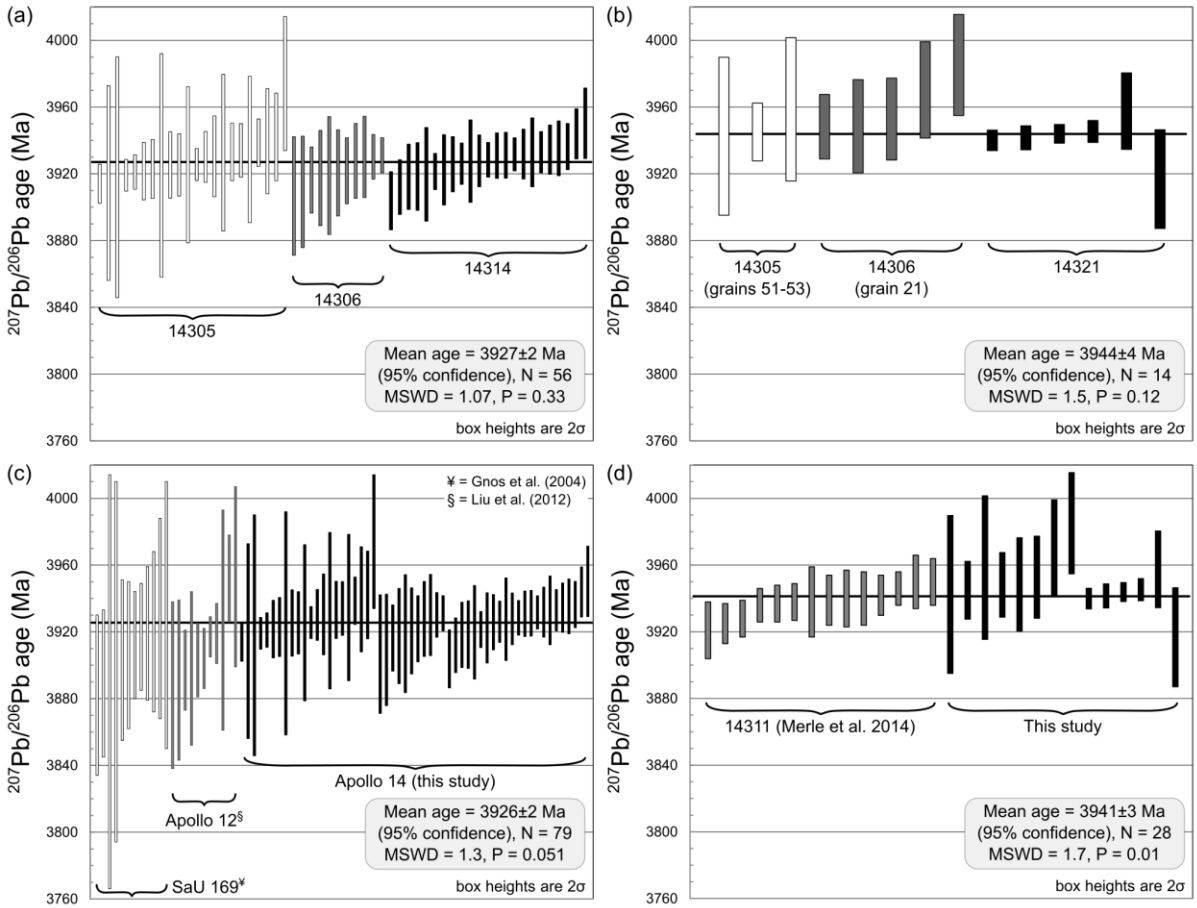

Figure 7. – Overview and combined weighted mean ages of (a) the younger and (b) older ^{207}Pb/^{206}Pb ages obtained for the Apollo 14 phosphates analysed in this study. Combined weighted mean ages have also been generated by comparing (c) the younger ages with the zircon ages obtained for Apollo 12 impact melt fragments and the lunar meteorite SaU 169 (Gnos et al. 2004; Liu et al. 2012), and (d) the older those determined for phosphates in 14311 by Merle et al. (2014).

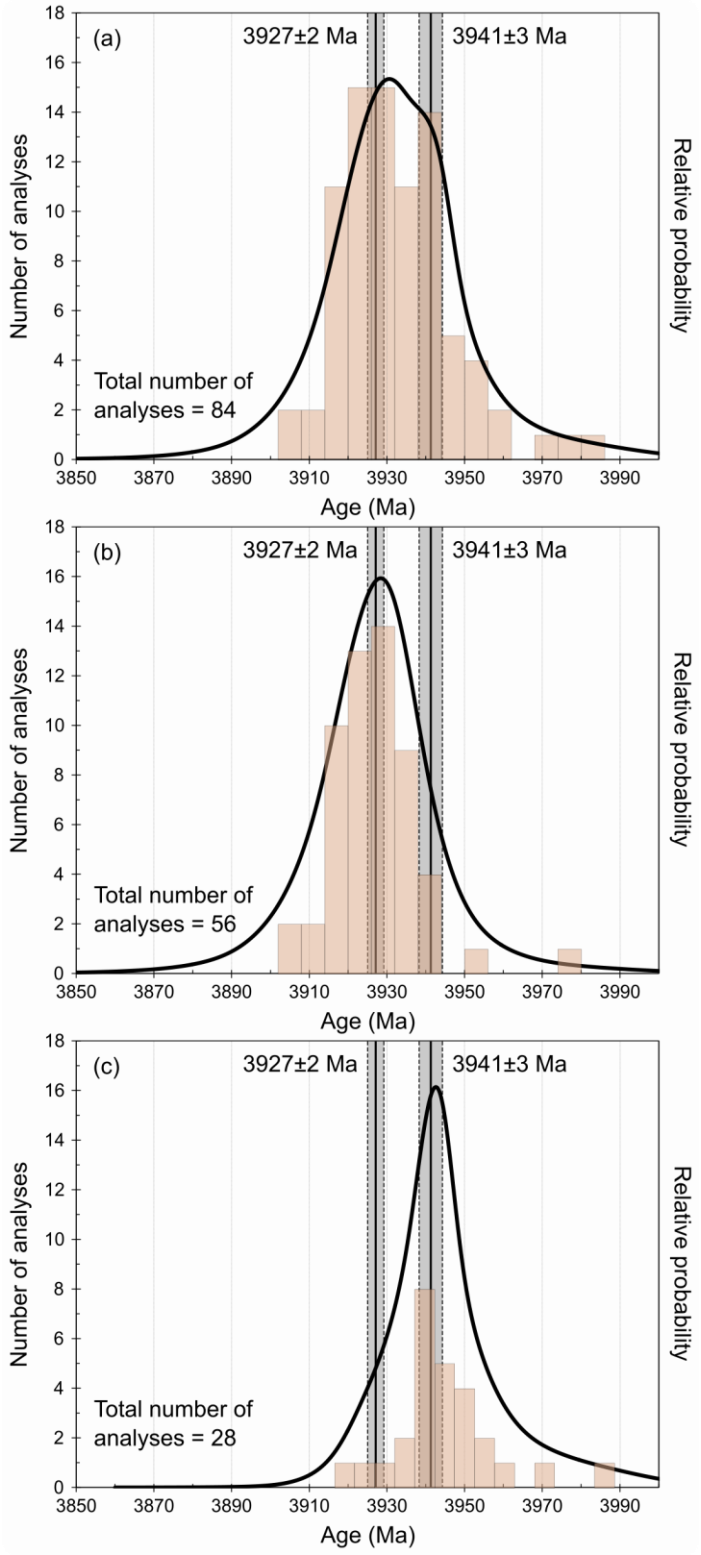

768

769 Figure 8. – Histograms and relative probability probability curves for: (a) all of the Apollo 14
770 phosphate $^{207}Pb/^{206}Pb$ ages presented in this study and by Merle et al. (2014); (b) the younger Apollo
771 14 phosphate $^{207}Pb/^{206}Pb$ ages from samples 14305, 14306 and 14314; and (c) the older Apollo 14
772 phosphate $^{207}Pb/^{206}Pb$ ages from this study and the data of Merle et al. (2014). The weighted mean
773 ages for the younger and older groups of phosphates have also been indicated on the plots.

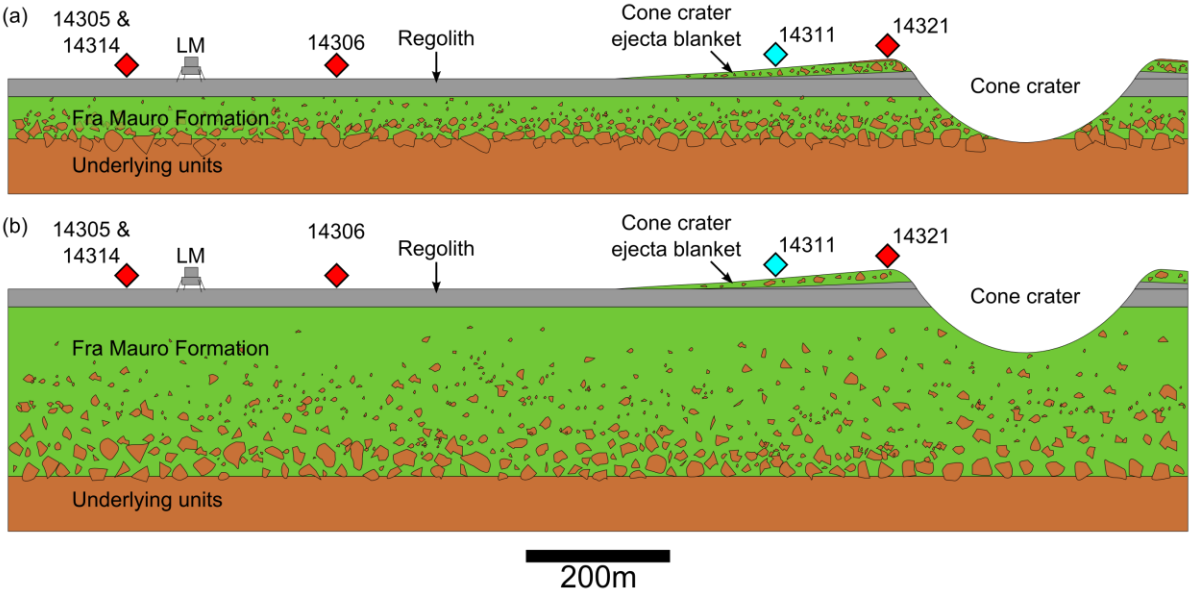

Figure 9. – Two hypothetical cross-sections of the Apollo 14 landing site illustrating the (a) lower and (b) upper estimates for the thickness of the Fra Mauro Formation (shown in green) based on the results of the Apollo 14 active seismic experiment (Watkins and Kovach 1972). The light brown, underlying unit, represents pre-Imbrian material, also found as clast within the Fra Mauro Formation. The grey unit represents the unconsolidated regolith. The depth of Cone Crater illustrated here does not represent the final crater depth, rather the estimated excavation depth according to canonically accepted crater scaling relationships (Melosh 1989). A 3× vertical exaggeration has been applied to both cross sections. Also indicated are the approximate locations from which the samples in this study (red diamonds) and 14311 (blue diamond; Merle et al. 2014) were collected. LM = location of the Lunar Module.

	$^{207}Pb/^{206}Pb$ ages			
Sample Number	**Age (Ma)**	**±**	**MSWD**	**P**
14305,103	3926	4	1.02	0.43
14306,150	3926	6	0.56	0.85
14314,13	3929	4	1.40	0.12
14321,134	3943	5	1.30	0.27
14305,103 - gr51-53	3946	15	0.19	0.83
14314,13 - gr21	3958	19	1.40	0.23

Average $^{207}Pb/^{206}Pb$ ages	$^{207}Pb/^{206}Pb$			
	Age (Ma)	**±**	**MSWD**	**P**
14305,103 **14306,150** **14314,13**	3927	2	1.07	0.33
14321,134 **14305,103 - gr51-53** **14314,13 - gr21**	3944	4	1.50	0.12

Table 1. – Summary of the $^{207}Pb/^{206}Pb$ ages obtained for the four samples.

Electronic Appendix

Figure A.1. – Back scattered electron (BSE) maps of: (a) 14305,103; (b) 14306,150; (c) 14314,13; and (d) 14321,134. The locations of the analysed grains have been indicated. In the cases of samples 14305,103 and 14321,134, examples of several clasts and areas of brecciated matrix have also been indicated.

Figure A.2. – Conventional U-Pb concordia diagrams for each of the samples with the apatite (blue) and merrillite (grey) phases highlighted.

Figure A.3. – Plot of U (µg/g) vs. Th (µg/g) for all of the analysed grains with the apatite (blue) and merrillite (red) phases highlighted.

Figure A.4. – Back scattered electron (BSE) images of the grains analysed (in addition to those pictured in Fig. 6). The analysed grains are all outlined with solid white lines. Dashed white lines indicate the edges of clasts in the breccias. The average $^{207}Pb/^{206}Pb$ ages of each grain have been also indicated (errors are stated at the 95% confidence level).

Table B.1. – Table of all the SIMS data acquired for the four samples.

Table B.2. – Results from calculating the radial diameters of ejecta blankets and thickness of ejecta deposits from impact crater and basin ejecta blankets, relative to the location of the Apollo 14 landing site.

Appendix C – Detailed evaluation of Ar-Ar and Rb-Sr literature data available for samples from the Apollo 14 mission.